https://doi.org/10.15407/ujpe70.6.355

S.E. ZELENSKY

Taras Shevchenko National University of Kyiv
(64/13, Volodymyrska Str., Kyiv 01601, Ukraine; e-mail: Zelensky@knu.ua)

ANISOTROPY OF LASER-INDUCED THERMAL EMISSION OF ROUGH CARBON SURFACES

In this paper, the visible thermal emission of carbon materials under the irradiation by nanosecond infrared laser pulses is investigated. For rough carbon surfaces, the experiments show that the pulse length of laser-induced thermal emission depends on the direction of observation. In particular, in the case of observation along the material's surface, the duration of the emission pulse is typically 20÷40% longer than in the direction perpendicular to the surface. For the explanation of the observed anisotropy of the kinetics of laser-induced thermal emission, a calculation model is proposed, which accounts for significant heterogeneity of pulsed laser heating of rough surfaces. The computer modeling predicts that peaks and valleys of the surface relief can be heated to significantly different local temperatures, and the temperature relaxation in the relatively hot peaks is longer than in the relatively cold valleys. As a result, when the laser-induced thermal emission is observed along the surface, the valleys are shadowed by the peaks, and this circumstance leads to the observed anisotropy of thermal emission kinetics. The results of the computer simulations with regard for the effect of shadowing are consistent with the results of measurements.

K e y w o r d s: anisotropy, laser-induced thermal emission, kinetics, rough surfaces, carbon.

1. Introduction

The thermal effect of laser radiation is the basis of numerous technologies of the laser processing of materials [1–9]. The power of modern laser systems is sufficient to implement a variety of technologies, from sophisticated methods of laser surgery to powerful laser weapons and laser fusion. Due to the well-known features of laser light sources, even not too powerful pulsed lasers (laboratory-scale lasers) are capable of producing sufficiently strong thermal effects. For example, when light-absorbing materials are irradiated with powerful laser pulses of the order of 10^{-8} s, thin surface layers of irradiated materials can be heated to temperatures of thousands of degrees. Under suchs, even the naked eye can observe a short flash of white glow of the irradiated surface. This laser-induced secondary radiation is thermal in nature and is well described by classical laws of thermal radiation, including Planck's formula for blackbody emission.

Despite the fact that the physical mechanism of the above-mentioned laser-induced thermal emission (LITE) is well-understood, the phenomenological properties of this emission are quite complex. In particular, when LITE is recorded in a narrow spectral interval (through a monochromator or a bandpass filter), its intensity depends nonlinearly on the intensity of laser excitation. In addition, the behaviors of the pulse amplitude and of the pulse energy are different, since the shape of emission pulses depends on the intensity of laser excitation. In typical cases, the emission pulse shape is asymmetrical. As a rule, the

C i t a t i o n: Zelensky S.E. Anisotropy of laser-induced thermal emission of rough carbon surfaces. *Ukr. J. Phys.* **70**, No. 6, 355 (2025). https://doi.org/10.15407/ujpe70.6.355.

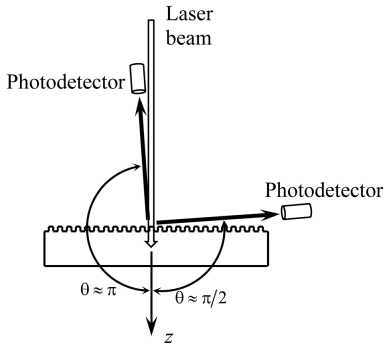

Fig. 1. The experiment layout

leading edge of LITE pulses is almost twice as short as the duration of the laser excitation pulse. As for the trailing edge, it can have a complex shape: in some cases, fast and slow components can be distinguished in the emission decay curve.

For the pulsed laser heating of surface layers of light-absorbing materials, the computer modeling shows that the characteristics of LITE are significantly affected by the roughness of the irradiated surface [10–13]: rough surfaces are heated non-homogeneously, and this fact affects the kinetics of thermal emission decay.

In this work, another unexplored property of LITE is considered. As the experiments show, the LITE pulse duration depends on the relative layout of the laser beam, of the irradiated surface, and of the direction of observation. Such anisotropy of LITE is observed on some rough light-absorbing surfaces. In this work, the anisotropy of LITE of rough carbon surfaces is investigated. To the author's knowledge, this anisotropy of LITE is observed for the first time.

2. Methods

The measurements of shape of LITE pulses were carried out as described in [13, 14] using a Q-switched YAG:Nd laser (wavelength 1064 nm, pulse length 20 ns), a high-speed photomultiplier H1949-51 (rise time 1.3 ns), and a digital oscilloscope (bandwidth 250 MHz). Glass filters were used for the selection of LITE emission in the spectral interval of 560 ± 20 nm. The power density of the laser radiation was $F_0 = 5 \div 10$ MW $\cdot$ cm^{-2} for different materials. The maximal surface temperature was estimated to be about 2500 ... 3000 K. The measurements were carried out in a single-pulse mode. The laser beam was directed perpendicular to the irradiated surface, while the observation direction was varied from the normal (almost reverse) ($\theta \approx \pi$, Fig. 1) to the tangential direction ($\theta \approx \pi/2$, Fig. 1).

The following carbon materials were used for measurements: spectroscopic-grade carbon electrodes, charcoal (oak), pharmaceutical porous activated carbon (in the form of tablets), and carbon-filled black paper. Typical SEM images of the samples are given in [13, 14]. Before the measurements, to remove moisture accumulated during storage, the samples were heated for 15 minutes to a temperature of about 150 °C. In addition, before the measurements, the samples were pre-irradiated with a sequence of 20 ... 30 laser pulses of increased intensity ($F_0 \approx$15 MW $\cdot$ cm^{-2}); such treatment significantly reduces the effects of the laser irradiation dose on the intensity and shape of LITE pulses [12]. All measurements were made at room temperature.

To calculate the shape of LITE pulsed signals of carbon materials, computer modeling of the dynamics of temperature field in the surface layer of the irradiated material was carried out using the classical equation of heat conduction, similarly to [13–15]. The emission signal was calculated using Planck's formula for blackbody thermal radiation in a narrow spectral interval. The calculations unvolved the porosity of the material, the presence of atmospheric air, as well as the temperature dependence of thermal characteristics of carbon and air (the coefficient of thermal conductivity and the specific heat capacity).

3. Results and Discussion

For the computer modeling of temperature distribution on a rough surface under the pulsed laser irradiation, the surface relief was presented as an ensemble of cylindrical protrusions (a single surface element is depicted in Fig. 2). A cylindrical coordinate system was used with z axis along the direction of propagation of the laser beam perpendicular to the irradiated surface. Assume that the diameter of the cylindrical protrusion is equal to its height, $2R_1 = h$, and also $R_2 = 2R_1$. Denote S_1 to be the area of the protrusion's top surface, $S_2 + S_3$ the area of the lateral cylindrical surface of the protrusion ($S_2 = S_3$), and S_4 the area of the valley around the protrusion.

As for the choice of specific values of the roughness element dimensions, as well as the ratio between them, it is worth noting the following consid-

erations. First, all the samples of carbon materials studied in the work had rough surfaces with roughness elements of various sizes and shapes, which creates conditions for observing the anisotropy of LITE on different samples. Second, as previous studies have shown, the inhomogeneity of heating of surface roughness elements during the pulsed laser irradiation is most pronounced in the case where the dimensions of the irradiated element correspond by order of magnitude to the characteristic distances determined by the depth of penetration of the laser radiation into the irradiated material, as well as the length of thermal diffusion in the material during the laser pulse. Finally, for computer modeling, such a ratio of the roughness element sizes was chosen, which allowed us to largely realize the inhomogeneity of its heating and to obtain the maximum difference in the shapes of LITE signals from different sections of the surface of the protrusions and depressions. Given the expected mechanism of LITE anisotropy, a surface element with the simplest shape was selected for the computer modeling to simplify calculations.

Consider the results of calculations for a material with a porosity of 74%, which corresponds to the above-mentioned pharmaceutical activated carbon. Figure 3 shows the results of calculations of the surface temperature T (Fig. 3, *b*) and of the surface exitance ϵ (Fig. 3, *c*) at point A (Fig. 2). Fig. 3, *a* demonstrates the shape of the laser pulse. The moment of time $t_{\max}$ corresponds to the maximal value of temperature (and, accordingly, the maximal value of exitance) at the selected point A at the top of the protrusion. The exitance ϵ (Fig. 3, *c*) is calculated according to Planck's formula in a narrow spectral interval around 560 nm, which corresponds to the experimental conditions.

As predicted in [11], for a pulsed laser irradiation of a rough surface, non-uniform heating of the surface relief elements can be expected. In particular, work [11] presents the results of calculations which predict the significant difference in temperature of peaks and valleys on the surface. It should be noted that the calculations in [11] were made without consideration of the temperature dependence of thermo-physical characteristics of the irradiated material. As is shown in [15], the account for the temperature dependence of the thermal conductivity and heat capacity of carbon is critically important for the correct description of the kinetics of LITE decay of such materials. In

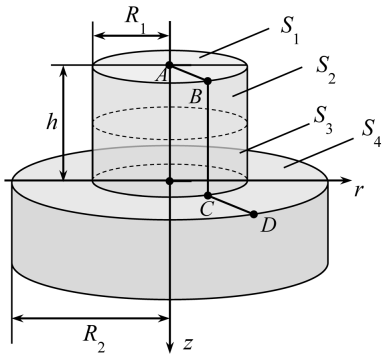

Fig. 2. Rough surface element model

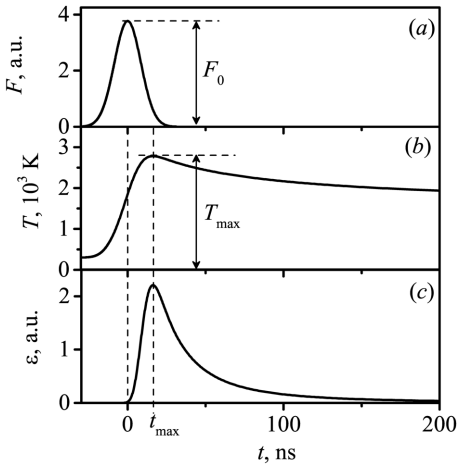

Fig. 3. The shape of the laser pulse (*a*) and the calculated time dependences of temperature (*b*) and exitance (*c*) at point A (Fig. 2)

particular, in the temperature range relevant for the observation of LITE, the thermal conductivity of carbon decreases by an order of magnitude (compared to the value at room temperature), which leads to the appearance of a slow component in the emission decay. As will be shown below, the anisotropy of LITE, which is studied in this work, is most pronounced just at the trailing edge of the emission pulse.

Fig. 4 shows the calculated temperature distribution along the line $ABCD$ (Fig. 2) on the surface at the moment $t_{\max}$ with regard for the temperature dependence of the coefficient of thermal conductivity κ and of the specific heat capacity c_p. As is seen from Fig. 4, the temperatures of different areas of the surface differ significantly. In particular, the areas distant from the vertical wall (for example, at the top surface, near point A, Fig. 2) have the highest tem-

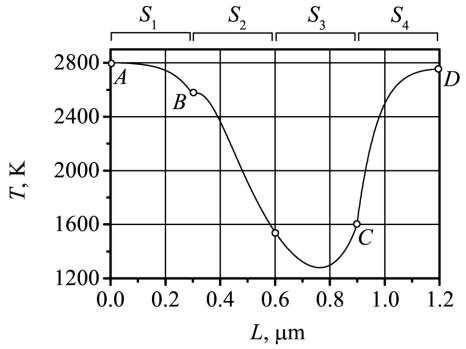

Fig. 4. Calculated temperature distribution along line $ABCD$ (Fig. 2) at the timepoint $t_{\max}$

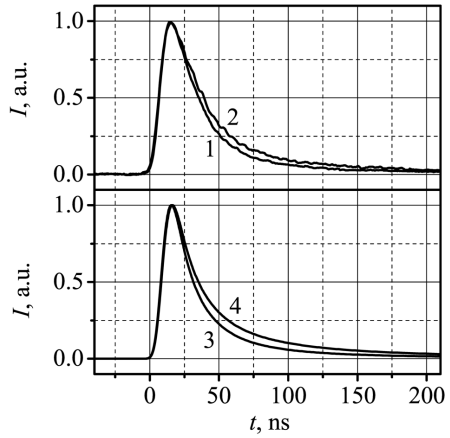

Fig. 5. Experimental normalized oscillograms of LITE of the activated carbon sample for $\theta \approx \pi$ (curve *1*) and $\theta \approx \pi/2$ (curve *2*) and calculated normalized oscillograms from areas $S_1 + S_2 + S_3 + S_4$ (curve *3*) and $S_1 + S_2$ (curve *4*)

perature, while the areas near the bottom of the wall (near point C) are less heated.

The shape of a thermal emission pulse depends on the kinetics of the temperature at the selected point on the surface. Hereinafter, we will focus on the trailing edge of the emission pulse, which is determined by the kinetics of temperature decay. As can be seen from Fig. 3, the stage of decay of LITE begins at the moment of time $t_{\max}$, when the laser pulse is almost ended. Therefore, the kinetics of temperature decay at a selected point on the surface will be determined (i) by the characteristics of the material (thermal conductivity coefficient, specific heat capacity), (ii) by their temperature dependences, and (iii) by the initial temperature distribution under the surface (at the moment $t_{\max}$). This initial subsurface temperature distribution depends on many factors, including the absorption coefficient at the laser wavelength. It should also be noted that the kinetics of temperature decay is different for different values of $T_{\max}$, which is manifested in the experiments as a dependence of the duration of LITE pulses on the energy density ($\mathrm{J \cdot cm^{-2}}$) of pulsed laser excitation.

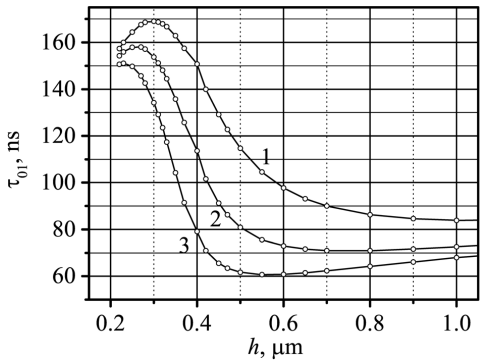

Fig. 6. Calculated values of LITE pulse width as a function of height of protrusions h for surface areas $S_1 + S_2$ (curve *1*), $S_1+S_2+S_3+S_4$ (curve *2*), S_3+S_4 (curve *3*) at $T_{\max} = 2800$ K at a wavelength of 560 nm

Thus, it can be expected that different areas of the irradiated rough surface will emit LITE signals, which differ not only by their amplitudes, but also by the pulse shapes. The integral LITE signal of the entire heterogeneously heated surface can be calculated by integrating the exitance ϵ over the area $S_1 + S_2 + S_3 + S_4$.

It should be emphasized that the experiments give the integrated emission signals from the surface areas that fall into the field of view of the photodetector. Consider the variants of relative position of the laser beam and of the direction of observation, shown in Fig. 1. If we place the photodetector so that the direction of observation is approximately opposite to the direction of the laser beam (Fig. 1, $\theta \approx \pi$), the thermal radiation will fall into the field of view of the photoreceptor mainly from areas S_1 and S_4, and partially from $S_2 + S_3$ (Fig. 2). If we place the photodetector with the direction of observation tangential to the surface (Fig. 1, $\theta \approx \pi/2$), the thermal radiation will fall into the field of view of the photodetector mainly from areas S_2 and partially S_1 (Fig. 2), while areas S_3 and S_4 will (at least partially) be overlapped (shadowed) by neighboring protrusions. Thus, for measurements performed in accor-

dance with Fig. 1, it can be expected that different shapes of LITE signals will be observed for $\theta \approx \pi$ and $\theta \approx \pi/2$.

The results of the corresponding calculations are shown in Fig. 5. Curve *3* in Fig. 5 is obtained by integrating the exitance ϵ within the area $S_1+S_2+S_3+S_4$, which approximately corresponds to the case $\theta \approx \pi$, and curve *4* is the result of the integration over $S_1 + S_2$, which approximately corresponds to $\theta \approx \pi/2$. As can be seen from the figure, the calculated emission pulses differ significantly.

Figure 5 also shows typical experimental oscillograms obtained on a sample of activated carbon. As is seen from Fig. 5, curves *1* and *2* are noticeably different, that is, the experiment confirms the presence of the anisotropy of LITE of the rough surface of the activated carbon sample. Similar results were obtained on all samples of carbon materials investigated in this work.

As is seen from Fig. 5, the difference between the emission pulses detected at different directions of observation is most pronounced at relatively far stage of the LITE decay. In view of this circumstance, for comparison of the results of calculations with the results of experiments, it seems convenient to measure the width of a LITE pulse at a level of 0.1 of its maximum (denote τ_{01}). Figure 6 shows the results of calculations for different possible values of height h of cylindrical protrusions on the surface (with the appropriate values of radius $R = h/2$). As is seen from Fig. 6, the thermal emissions from different areas $S_1 \div S_4$ have significantly different values of the a pulse width τ_{01}.

The results of measurements are given in Table. As is seen from Table and Fig. 6, the values of τ_{01} observed in the experiments satisfactorily correspond to the results of calculations in the interval of $h = 0.55 \div 0.65$ μm.

Measured LITE pulse width

Material	τ_{01}, ns	
	$\theta \approx \pi$	$\theta \approx \pi/2$
Activated carbon	77	92
Charcoal	78	90–100
Carbon electrode	52	70
Carbon-filled paper	92	142

The consistency of the results shown in Fig. 6 and in Table testifies in favor of the proposed mechanism of anisotropy of LITE of rough surfaces.

At the end, it should also be noted that the geometric model of LITE anisotropy considered in this work is partially similar to the thermophysical models that describe the heating and thermal radiation of surfaces of atmosphereless planetary astronomical objects with topographic features [16–18] and of the Earth's surface [19–21]. In the above-mentioned thermophysical models, the key role is played by the effect of shading of some areas on the surface. As a consequence, peculiarities are observed in the propagation of radiation in directions along the surface, and, for example, cold traps for water can be formed in the permanently shadowed regions at the south pole of the Moon [16].

4. Concluding Remarks

Summing up, it is worth paying attention to the following circumstances. The experiments with the laser-induced thermal emission of rough surfaces have shown that the differences in widths of the emission pulses reach 20–40% on all examined samples. Such a significant effect needs to be taken into account both during the measurements and in the corresponding calculations. Therefore, the results obtained in this work deepen the understanding of the processes of laser heating of rough light-absorbing surfaces and will contribute to the development of more advanced models of the formation of pulsed thermal emission signals. In addition, it is possible that the revealed effect of anisotropy of laser-induced thermal emission kinetics can be used for monitoring of changes of surface roughness during laser processing, but this issue requires separate study.

The work was carried out with the support of the Ministry of Education and Science of Ukraine in accordance with Agreement No. BF/30-2021 dated August 4, 2021.

1. C.Y. Yap, C.K. Chua, Z.L. Dong, Z.H. Liu, D.Q. Zhang, L.E. Loh, S.L. Sing. Review of selective laser melting: Materials and applications. *Appl. Phys. Rev.* **2**, 041101 (2015).
2. P. Hildinger, T. Seefeld, A. Bohlen. Characterization of optical emissions during laser metal deposition for the implementation of an in-process powder stream monitoring. *J. Laser Appl.* **35**, 042048 (2023).

3. Z. Yan, W. Liu, Z. Tang, X. Liu, N. Zhang, M. Li, H. Zhang. Review on thermal analysis in laser-based additive manufacturing. *Optics and Laser Technology* **106**, 427-41 (2018).
4. T. Shimotsuma, A. Geshiro, M. Tsuyama, M. Heya, H. Nakano. Double-pulse laser peening as a surface enhancement technology. *J. Laser Appl.* **36**, 042064 (2024).
5. E. Khalkhal, M. Rezaei-Tavirani, M.R. Zali, Z. Akbari. The evaluation of laser application in surgery: A review article. *J. Lasers in Med. Sci.* **10** (Suppl. 1), S104 (2019).
6. M. Bachmann, A. Artinov, X. Meng, S.N. Putra, M. Rethmeier. Challenges in dynamic heat source modeling in high-power laser beam welding. *J. Laser Appl.* **35**, 042003 (2023).
7. X. Zhang, C.J. Yocom, B. Mao, Y. Liao. Microstructure evolution during selective laser melting of metallic materials: A review. *J. Laser Appl.* **31**, 031201 (2019).
8. L. Hou, F. Yin, S. Wang, J. Sun, H. Yin. A review of thermal effects and substrate damage control in laser cleaning. *Optics and Laser Technology* **174**, 110613 (2024).
9. O. Ashraf, N.V. Patel, S. Hanft, S.F. Danish. Laser-induced thermal therapy in neuro-oncology: A review. *World Neurosurgery* **112**, 166 (2018).
10. S.E. Zelensky, L.V. Poperenko, A.V. Kopyshinsky, K.S. Zelenska. Nonlinear characteristics of laser-induced incandescence of rough carbon surfaces. *Proc. SPIE* **8434**, 8434H-1-6 (2012).
11. K.S. Zelenska, S.E. Zelensky, A.V. Kopyshinsky, S.G. Rozouvan, T. Aoki. Laser-induced incandescence of rough carbon surfaces. *Japanese J. Appl. Phys.: Conf. Proc.* **4**, 011106-1-6 (2016).
12. V. Karpovych, K. Zelenska, S. Yablochkov, S. Zelensky, T. Aoki. Evolution of laser-induced incandescence of porous carbon materials under irradiation by a sequence of laser pulses. *Thai J. Nanosci. Nanotechnol.* **2** (2), 14 (2017).
13. V. Karpovych, O. Tkach, K. Zelenska, S. Zelensky, T. Aoki. Laser-induced thermal emission of rough carbon surfaces. *J. Laser Appl.* **32**, 012010 (2020).
14. S.E. Zelensky, T. Aoki. Decay kinetics of thermal emission of surface layers of carbon materials under pulsed laser excitation. *Optics and Spectroscopy* **127**, 858 (2019).
15. S. Zelensky, O. Kolesnik, V. Yashchuk. The role of air in laser-induced thermal emission of surface layers of porous carbon materials. *Ukrainian J. Phys.* **68** (10), 652 (2023).
16. D.A. Paige, M.A. Siegler, J.A. Zhang, P.O. Hayne, E.J. Foote, K.A. Bennett, A.R. Vasavada, B.T. Greenhagen, J.T. Schofield, D.J. McCleese, M.C. Foote, E. Dejong, B.G. Bills, W. Hartford, B.C. Murray, C.C. Allen, K. Snook, L.A. Soderblom, S. Calcutt, F.W. Taylor, N.E. Bowles, J.L. Bandfield, R. Elphic, R. Ghent, T.D. Glotch, M.B. Wyatt, P.G. Lucey. Diviner lunar radiometer observations of cold traps in the Moon's south polar region. *Science* **330** (6003), 479 (2010).
17. B. Rozitis, S.F. Green. Directional characteristics of thermal-infrared beaming from atmosphereless planetary surfaces – a new thermophysical model. *Monthly Notices of the Royal Astronomical Society* **415** (3), 2042 (2011).
18. T.J. Warren, N.E. Bowles, H.K. Donaldson, J.L. Bandfield. Modeling the angular dependence of emissivity of randomly rough surfaces. *J. Geophysical Research: Planets* **124**, 585 (2019).
19. E.S. Krayenhoff, J.A. Voogt. Daytime thermal anisotropy of urban neighbourhoods: Morphological causation. *Remote Sens.* **8** (2),108 (2016).
20. D. Wang, Y. Chen, I. Hu, J.A. Voogt, X. He. Satellite-based daytime urban thermal anisotropy: A comparison of 25 global cities. *Remote Sensing of Environment* **283**, 113312 (2022).
21. B. Cao, Q. Liu, Y. Du, J.-L. Roujean, J.-P. Gastellu-Etchegorry, I.F. Trigo, W. Zhan, Y. Yu, J. Cheng, F. Jacob, J.-P. Lagouarde, Z. Bian, H. Li, T. Hu, Q. Xiao. A review of Earth surface thermal radiation directionality observing and modeling: Historical development, current status and perspectives. *Remote Sensing of Environment* **232**, 111304 (2019).

Received 27.01.25

С.Є. Зеленський

АНІЗОТРОПІЯ ІНДУКОВАНОГО ЛАЗЕРОМ ТЕПЛОВОГО ВИПРОМІНЮВАННЯ ШОРСТКИХ ВУГЛЕЦЕВИХ ПОВЕРХОНЬ

У даній роботі досліджено видиме теплове випромінювання вуглецевих матеріалів при опроміненні інфрачервоними лазерними імпульсами наносекундної тривалості. Для шорстких вуглецевих поверхонь експерименти показують, що тривалість імпульсу індукованого лазером теплового випромінювання залежить від напрямку спостереження. Зокрема, при спостереженні вздовж поверхні матеріалу тривалість імпульсу випромінювання зазвичай на 20–40% більша, ніж у напрямку, перпендикулярному до поверхні. Для пояснення спостережуваної анізотропії кінетики лазерно-індукованого теплового випромінювання запропоновано розрахункову модель, яка враховує значну неоднорідність імпульсного лазерного нагріву шорстких поверхонь. Комп'ютерне моделювання передбачає, що вершини та западини рельєфу поверхні можуть бути нагріті до суттєво різних локальних температур, а температурна релаксація у відносно гарячих піках довша, ніж у відносно холодних долинах. Як наслідок, коли індуковане лазером теплове випромінювання спостерігається вздовж поверхні, долини затіняються піками, і ця обставина приводить до спостережуваної анізотропії кінетики теплового випромінювання. Результати комп'ютерного моделювання з урахуванням ефекту затінення узгоджуються з результатами вимірювань.

Ключові слова: анізотропія, індуковане лазером теплове випромінювання, кінетика, шорсткі поверхні, вуглець.